



Crude oil burning mechanisms

A conceptual model review

van Gelderen, Laurens; Malmquist, L.M.V.; Jomaas, Grunde

Published in:

Proceedings of the 38th AMOP Technical Seminar on Environmental Contamination and Response

Publication date:

2015

Document Version

Peer reviewed version

[Link back to DTU Orbit](#)

Citation (APA):

van Gelderen, L., Malmquist, L. M. V., & Jomaas, G. (2015). Crude oil burning mechanisms: A conceptual model review. In Proceedings of the 38th AMOP Technical Seminar on Environmental Contamination and Response

DTU Library

Technical Information Center of Denmark

General rights

Copyright and moral rights for the publications made accessible in the public portal are retained by the authors and/or other copyright owners and it is a condition of accessing publications that users recognise and abide by the legal requirements associated with these rights.

- Users may download and print one copy of any publication from the public portal for the purpose of private study or research.
- You may not further distribute the material or use it for any profit-making activity or commercial gain
- You may freely distribute the URL identifying the publication in the public portal

If you believe that this document breaches copyright please contact us providing details, and we will remove access to the work immediately and investigate your claim.

Crude Oil Burning Mechanisms: A Conceptual Model Review

Laurens van Gelderen^{a*}, Linus M.V. Malmquist^b, Grunde Jomaas^a
^aDepartment of Civil Engineering, Technical University of Denmark

^aKgs. Lyngby, Lyngby-Taarbæk, Denmark

^bDepartment of Plant and Environmental Sciences, University of Copenhagen

^bFrederiksberg, Frederiksberg C, Denmark

* Email: Lauge@byg.dtu.dk.

Abstract

In order to improve predictions for the burning efficiency and the residue composition of *in-situ* burning of crude oil, the burning mechanism of crude oil was studied in relation to the composition of its hydrocarbon mixture, before, during and after the burning. The surface temperature, flame height, mass loss rate and residues of three hydrocarbon liquids (*n*-octane, dodecane and hexadecane), two crude oils (DUC and REBCO) and one hydrocarbon liquid mixture of the aforementioned hydrocarbon liquids were studied using the Crude Oil Flammability Apparatus. The experimental results were compared to the predictions of four conceptual models that describe the burning mechanism of multicomponent fuels. Based on the comparisons, hydrocarbon liquids were found to be best described by the Equilibrium Flash Vaporization model, showing a constant gas composition and gasification rate. The multicomponent fuels followed the diffusion-limited gasification model, showing a change in the hydrocarbon composition of the fuel and its evaporating gases, as well as a decreasing gasification rate, as the burning progressed. This burning mechanism implies that the residue composition and burning efficiency mainly depend on the highest achievable oil slick temperature. Based on this mechanism, predictions can then be made depending on the hydrocarbon composition of the fuel and the measured surface temperature.

Glossary

| | | | |
|--------------|------------------------------------|-------------|--|
| BE | Burning Efficiency | \dot{m} | Mass Loss Rate (g/s) |
| COFA | Crude Oil Flammability Apparatus | Pe_m | Peclet Number for Mass Diffusion (-) |
| DLG | Diffusion-Limited Gasification | \dot{Q}_c | Energy Release Rate from Combustion (kW) |
| EFV | Equilibrium Flash Vaporization | | |
| FID | Flame Ionization Detector | \dot{Q}_F | Energy Release Rate from the Flame to the Fuel Surface (kW) |
| GC | Gas Chromatography | | |
| HCL | Hydrocarbon Liquid | \dot{Q}_L | Energy Release Rate Losses to the Water Layer (kW) |
| ISB | <i>In-Situ</i> Burning | | |
| PGC | Pyrex Glass Cylinder | T_b | Boiling Point (K) |
| D | Diameter (m) | T_s | Surface Temperature (K) |
| ΔH_c | Heat of Combustion (kJ/kg) | $T_{s,i}$ | Surface Temperature After the Initial Startup Phase of the Burning (K) |
| ID | Internal Diameter (m) | | |
| L_F | Flame Height (m) | χ | Combustion Efficiency Factor (-) |
| L_v | Latent Heat of Evaporation (kJ/kg) | | |

1 Introduction

In the Arctic, oil spills pose an upcoming threat to its environment due to the increasing amount of marine transportation and oil exploration (AMAP, 2010a). The remoteness and extreme climate of Arctic waters make it more difficult for conventional oil spill response methods to be deployed effectively (Fitzpatrick, 1985; Nuka Research & Planning Group, 2010). A promising response method suitable under these circumstances is the *in-situ* burning (ISB) of the crude oil on the water surface. This technique features simple logistics, can be used in ice-infested waters and can obtain a high efficiency (Buist et al., 1999; Nordvik, 1995). The parameter mostly determining the effectiveness of ISB is the burning efficiency (BE), i.e. the amount of oil (in wt. %) that is removed from the water surface during the burning. In order to establish whether or not ISB is a favorable response method for Arctic oil spills, it is therefore relevant to be able to predict the BE under a wide range of conditions.

Experimental research has shown a wide spread in BEs which could not be related directly to the used variety of oils, burning conditions and pool sizes. Large scale experiments that have been conducted on open water (with and without ice) showed the highest BEs, reaching up to 99% (Allen, 1990; Brandvik et al., 2010; Fingas et al., 1994; Potter, 2010). Small scale experiments with similar crude oils showed much lower BEs as low as 40% (Farmahini Farahani et al., 2015; Fritt-Rasmussen and Brandvik, 2011; Fritt-Rasmussen et al., 2012). These results seem to suggest that large scale experiments have higher BEs than small scale, which would inherently improve the potential of ISB as a response method. However, the main focus of these experiments was on the practical aspects of ISB and limited theoretical knowledge on the burning mechanism of crude oils that determine the BE has been acquired. If the lower BEs observed for smaller scale experiments would be representative for full scale operations, ISB might not be an attractive response method for certain oils. As such, a better understanding of the burning mechanisms is desirable to allow for the proper interpretation of scaled ISB experiments and as a result improve BE predictions. In addition, mechanistic insight can provide information on the composition of the residue that is formed during the burning, which also plays a role in determining the effectiveness of ISB.

The main challenge in determining the burning mechanism of crude oils comes from the fact that they consist of many hundreds of different hydrocarbons, each with their own specific flash point, boiling point, viscosity, etc. (AMAP, 2010b; Fingas, 2011b). It is not well-understood how each individual compound affects the whole system and what happens with each individual compound when a crude oil is ignited. Considering that it is not the liquid oil itself that is burning, but rather the gases evaporating from the oil slick, the oil composition can vary from the composition of the flammable gases. For a compound inside an oil to evaporate, it must be physically near the liquid surface. This means that compounds ‘trapped’ in the bottom of an oil slick cannot burn no matter the burning conditions. Hence, it is crucial to understand which hydrocarbons contribute to the composition of the flammable gases as a function of time. When this is known, it becomes easy to deduce the compounds that will end up forming the residue and thus what the BE will be.

Herein, the goal is to establish a model that describes the gasification process of burning crude oil and thus its burning mechanism, based on previous proposed models and experimental observations. Over the past decades a number of models have been proposed that described the burning of oil mixtures. The next section will give a short overview of the models that can be applied to the ISB of crude oils. These models are then compared to a series of experimental observations in order to establish a model for the burning mechanism of crude oil.

1.1 Model Review

In the latest review on ISB, the *Equilibrium Flash Vaporization* (EFV) model was proposed for the burning mechanism of crude oil (Buist et al., 2013), which has been observed earlier by Petty (1983). This model describes the gasification of a multicomponent fuel as being of “essentially constant composition” (Petty, 1983) with a constant gasification rate. In other words, the many compounds in the fuel behave as one compound with an ‘average’ flashpoint and boiling point. Characteristics of this model are that the crude oil should burn with constant surface temperature at a constant burning rate, have a temperature gradient in the oil slick and allow for lighter components to be present in the residue (Buist et al., 2013; Petty, 1983).

An alternative to the EFV model was proposed by Buist et al. (1997), based on their studies on crude oil residues. Their results showed that crude oil residues had an increased concentration of heavy hydrocarbon fractions (boiling point (T_b) >538 °C) and complete removal of the light hydrocarbon fractions (T_b <204 °C). The authors suggested that the burning proceeded according to an Imperfect EFV mechanism where lighter oil fractions are favored in the burning over heavier oil fractions. This implies that the gasification rate and composition is still constant, but that its composition differs from the crude oil composition.

Furthermore, three models have been developed for the combustion of multicomponent fuels based on the Peclet number for mass diffusion (Pe_m), Eq. (1), (Law, 2006). The value of Pe_m determines which of these three models is the most appropriate to describe the gasification of the certain fuel (Makino and Law, 1988). While these models have not been developed directly for the burning of crude oils, they describe the interaction between a multicomponent fuel and its evaporating gases in great detail.

$$Pe_m = \frac{K}{D_l} = \frac{\text{gasification rate}}{\text{mass diffusion rate}} \quad (1)$$

For fuels where Pe_m approaches infinity, most likely due to negligible mass diffusion, e.g. in solids, the composition of the fuel is fixed and no internal changes occur during the combustion. This means that the fuel is burned layer by layer and hence this model is known as the *Onion Skin model*. For fuels where Pe_m approaches zero, the fuel can be considered to have a uniform distribution of its components, due to its relatively high mass diffusion rate. Hence, the gasification of gases on its surface depends only on relative volatility differences of the compounds. This model is known as the *Batch Distillation model* and describes the fuel as being burned compound by compound with decreasing volatility (Law, 1976).

For fuels with a low Pe_m value ($\ll 1$), the gasification is controlled by boundary layers (Law, 1978; Wang et al., 1984). At the start of the combustion, the most volatile compound at the surface will determine the gasification rate by its volatility, like the batch distillation model. When the concentration becomes too low to support this gasification rate, gasification becomes controlled by the mass diffusion rate of this compound. Since mass diffusion is much slower, the less volatile compounds at the surface will also be able to contribute significantly to the gasification rate. Once the fuel becomes so thin that the fuel surface crosses the concentration boundary layer, the gasification rate becomes volatility controlled again. This causes a rapid depletion of the more volatile compounds and a quick increase in temperature as the less volatile compounds start to burn thereafter, until the fuel is fully consumed. For fuels several millimeters thick, this means that the majority of the time the evaporating gases have a mixed composition of compounds with similar T_b . In this study, we will refer to this model as the *diffusion-limited gasification (DLG) model*.

Of these five models, the Onion Skin model is very unlikely to describe crude oil combustion, considering that crude oils do not show any solid-like behavior. It would require the crude oil to have either a near infinite gasification rate or near zero mass diffusion rate, both of which are implausible because crude oils consist of both light (high mass diffusion rate) and heavy hydrocarbons (low gasification rate). Therefore, the onion skin model is not considered to be a valid description of crude oil combustion.

The remaining four models present plausible, yet very different mechanisms for the combustion of crude oils; both the predicted residue compositions and the resulting BE vary for each model. As such, the uncertainties in ISB predictions based on any of these models would be numerous. In order to determine if one of these models or combination of models can accurately predict the gasification process and the related burning mechanism for crude oil, results of a series of small scale ISB experiments were compared to the model predictions. In the burning experiments of HCLs and crude oils on water, the surface temperature (T_s), mass loss rate (\dot{m}), flame height (L_F) and the residue composition were studied. Based on the comparison between experimental and modeled results a conceptual model for the burning mechanism of crude oil was established.

2 Materials and Methods

All experiments were performed in the Crude Oil Flammability Apparatus (COFA), following the procedures described in Van Gelderen et al. (2015) and hence only a short description of the procedures is given here. For measuring the surface temperature and flame height a Pyrex Glass Cylinder (PGC) of 160 mm diameter on an open metal foot was placed in a 1 x 1 x 0.5 m water basin to contain the oil. The open foot allowed for water to move freely at the bottom of the PGC to maintain the level of the oil surface constant for a longer period of time. For the mass loss rate, the PGC was placed on an open foot in a 0.3 x 0.3 x 0.4 m metal bucket filled with water, which stood on a scale that had a reading interval of 1 g. For all experiments, a known amount of oil, corresponding to an initial thickness of 5-40 mm, was poured carefully on the water in the PGC. A thermocouple array was then placed in position to measure the temperature at the oil surface and at 2, 3, 5, 10, 20, 30, 40, and 50 mm below the surface. A camera was used to capture the flame height after the oil was ignited with a butane blow torch. After the flame extinguished, the residue was collected with hydrophobic absorption pads and weighed.

To measure the burning parameters, three hydrocarbon liquids (HCLs) (*n*-octane, dodecane and hexadecane), a 1:1:1 volumetric ratio mixture of the HCLs and two crude oils (DUC, a North Sea crude and REBCO, a Russian Export Blend crude) were used. Oil characteristics of the oils are shown in Table 1. HCL and crude oil experiments were conducted with initial slick thicknesses of 10, 20 and 40 mm. Experiments with the HCL mixture were conducted with initial slick thicknesses of 15 and 30 mm and the mixture was homogenized before it was poured onto the water. Thin initial slick thicknesses (10-15 mm) had less height difference in oil surface level, so it was easier to measure the surface temperature, whereas the thicker slicks (20-40 mm) provided better results for the flame height and mass loss.

Gas Chromatography (GC) analysis with a Flame Ionization Detector (FID) was used to characterize the crude oil composition of DUC and REBCO and the residue composition of the HCL mixture and REBCO. The samples were analyzed on an Agilent 6890 GC-FID equipped with a 7683 autosampler and a 30 m ZB5 column (0.25 mm internal diameter (*ID*) and 0.25 μm film thickness). The inlet temperature was 310 °C and 1 μL was injected in split mode (5:1) held

for 2 min to a liner (4 mm *ID*) with a fixed plug of glass wool. Hydrogen was used as carrier gas with a flow rate of 2.0 mL/min and the detector setup was: a temperature 300 °C, hydrogen flow rate 35 mL/min, air flow 350 mL/min and nitrogen makeup flow of 40 mL/min. The initial oven temperature (40 °C) was held for 2 min, then increased to 310 °C at a rate of 15 °C/min (held for 10 min), leading to a total analysis time of 30 min. Peak identification was based on the two doubles pattern of heptadecane-pristane and octadecane-phytane (Fingas, 2011a; Stauffer et al., 2008).

3 Results and Discussion

3.1 Model Predictions

For each model, a set of qualitative predictions were made for T_s , \dot{m} , L_F and residue compositions of a crude oil burning on water (Figure 1). Although the models lack the numerical details that would allow for quantitative predictions, the qualitative results are still useful when compared to experimental results. In the EFV model, the constant nature of the gas composition and gasification rate results in constant burning parameters. The crude oil burns essentially as if it consisted of only one component, i.e. like a HCL. The T_s and L_F will likely lie in the range of the middle hydrocarbon fraction (T_b of 204-538 °C) (Buist et al., 1997), corresponding to the ‘averaged’ character of the flammable gases that consist of the full range of hydrocarbons present in the crude oil. Residues will more or less show the same composition as the crude oil, depending on the exact composition of the evaporating gases.

The Imperfect EFV model also uses a constant gasification rate and constant gas composition, but the composition of the gas is no longer similar to the crude oil composition due to its higher concentration of light hydrocarbons. This results in a lower T_s , higher L_F and \dot{m} (as explained below) and formation of a residue without a light hydrocarbon fraction (Buist et al., 1997). The presence or absence of lighter hydrocarbons in the residue composition is the main parameter to distinguish between the EFV and Imperfect EFV model.

Both the Batch Distillation and DLG model feature the increased contribution of heavier hydrocarbon fractions to the gasification as the burning progresses, which results in more dynamic burning parameters. With increasing molecular weight, hydrocarbons generally show an increase in T_b and latent heat of evaporation (L_v) and a decrease in the heat of combustion (ΔH_c). The increasing T_b will directly reflect on the T_s and will show an increase of T_s over time (Figure 1). The models can be distinguished by the initial value of T_s after the initial startup phase of the burning ($T_{s,i}$). For the Batch Distillation model, the $T_{s,i}$ will correspond to that of the hydrocarbon with lowest T_b , which is usually around C₇ ($T_b = 98$ °C). The DLG model on the other hand will show a higher $T_{s,i}$ as the evaporating gases are composed of a mixture of several light fraction hydrocarbons.

The respective reduction and increase of ΔH_c and L_F affect the \dot{m} and L_F through a number of closely connected equations (Eq. (2), (3), (4) & (5)) (Drysedale, 2011).

$$\dot{Q}_c = \chi * \dot{m} * \Delta H_c \quad (2)$$

$$L_F = 0.23\dot{Q}_c^{2/5} - 1.02D \quad (3)$$

$$\dot{m} = \frac{\dot{Q}_F - \dot{Q}_L}{L_v} \quad (4)$$

$$\dot{m} = 0.076\dot{Q}_c^{1/3}L_F^{5/3} \quad (5)$$

Here \dot{Q}_c is the energy released in the flame, χ a factor that accounts for incomplete combustion, D the diameter of the pool, \dot{Q}_F the energy released from the flame to the fuel and \dot{Q}_L the energy release lost through the fuel surface to the water layer. When ΔH_c decreases, \dot{Q}_c decreases as well, considering that \dot{m} will not increase spontaneously for less volatile heavy hydrocarbons (Eq. (2)). Equation (3) shows that a decrease in \dot{Q}_c will lower L_F . As a consequence, \dot{Q}_F and \dot{Q}_L cannot make up for the reduction in \dot{m} caused by the increase in L_v and \dot{m} will thus decrease as well (Eq. (4)). This reduction in \dot{m} will further reduce \dot{Q}_c , resulting in a feedback loop until a new equilibrium between \dot{m} , \dot{Q}_c and L_F is reached (Eq. (5)). Thus, the contribution of heavier hydrocarbons results in a decreasing \dot{m} and L_F over time in both models, with a somewhat lower starting value for the DLG model due to the contribution of heavier hydrocarbons in the evaporating gases. The reduction in \dot{m} and L_F will be faster for the Batch Distillation model than for the DLG model as the composition of the evaporating gases changes more abruptly (Figure 1).

Regarding the residue composition, the Batch Distillation and DLG models once more provide similar predictions. Both models predict the complete removal of the light and most of the medium hydrocarbon fraction. The DLG model will show a gradual increase of the heavier hydrocarbon fraction, much like the Imperfect EFV model, as the heavier hydrocarbons contribute less and less to the gasification. On the other hand, the Batch Distillation model shows a more abrupt increase in concentration going rapidly from the last fraction that took part in the burning to the fraction that did evaporate at all. Figure 1 gives a visual representation of this behavior based on the GC spectrum of REBCO. Note that these spectra do not represent actual concentrations, only the relative residue composition for each model. In practice, it will be more difficult to discern between the Imperfect EFV, Batch Distillation and DLG model based on the residue composition of a crude oil. Still, all three models show a similar pattern: depletion of the lighter hydrocarbon fractions and increased concentrations of the heavier fractions.

As can be seen from Figure 1, the model predictions clearly show the distinction between either EFV and Imperfect EFV or Batch Distillation and DLG as model for crude oil combustion. Constant values for the T_s , \dot{m} and L_F indicate that one of the EFV models is followed, whereas dynamic values imply either the Batch Distillation or DLG model. To discern an individual model in these subdivisions, the residue composition and surface temperature can be used as discussed above.

3.2 Experimental Results

The results of the T_s measurements for the oil-on-water burning experiments are shown in Figure 2. The data shown is up to the point where the surface thermocouple was no longer attached to the surface due to thinning of the slick as the burning progresses. Comparison of Figure 1 and Figure 2 clearly shows that the EFV predictions match with the HCL data, showing nearly constant surface temperatures close to the respective T_b for the HCLs. Hexadecane proved very difficult to ignite as it suffered from significant heat losses to the water, which is reflected in the scattered T_s data. The T_s of the HCL mixture and crude oils increased steadily as a function of time, which matches with the predictions of the Batch Distillation and DLG model. A $T_{s,i}$ around 230 °C was observed for the multicomponent fuels, which indicates that the initial evaporating gases also included heavier hydrocarbons than just the lightest hydrocarbons present

in the fuel (C_6 - C_8 have a T_b of 69-126 °C, see Figure 4 for the hydrocarbon composition of REBCO). Therefore, the most accurate predictions for the T_s of multicomponent fuels are made by the DLG model.

Similar correspondence to the model predictions were found for the results of the flame height and mass loss rate (Figure 3). The results shown were obtained for initial slick thicknesses of 40 mm (*n*-octane, dodecane, DUC and REBCO), 30 mm (HCL mixture) and 20 mm (hexadecane). Each data point represents an averaged value over approximately 2% of the burning time. The presented flame height data points represent averages of 10 obtained flame height data points (see Van Gelderen et al. (2015)). Mass loss rates were averaged over the same time period (30-60 seconds) as the corresponding flame height intervals. The values reported here were not corrected for any water mass losses, which have been shown to influence the averaged burning rate (Van Gelderen et al., 2015). However, any corrections for water mass losses did not alter the observed trends in the data and thus were not taken into account to avoid additional uncertainties.

The HCLs followed the L_F predictions of the EFV models reasonably, with only a minor decrease in L_F over time. This was most likely caused by increasing heat losses to the water as the slick becomes thinner, which leads to an increase in \dot{Q}_L . Semi-constant values were also observed for the \dot{m} of *n*-octane and hexadecane. Scatter in the data is mainly caused by the lower amount of mass used, respectively due to a lower density and thinner slick thickness, but the general pattern still matched the EFV predictions. Contrary, the increasing \dot{m} of dodecane does not match with any of the described models, nor matches with the decreasing L_F in conjunction with Equations (2) & (3). The phenomenon is possibly caused by some unknown interaction with the surrounding water, though as mentioned, adjusting for the water mass losses did not alter the increasing trend of \dot{m} . No explanation could be found for this increase in \dot{m} in the current data and further research was beyond the scope of this study. Overall, the L_F and \dot{m} results for the HCLs are best described by the EFV models, as expected.

Contrary to the T_s results (Figure 2), the L_F and \dot{m} of the HCL mixture do not show data that clearly suggest a certain burning mechanism. For both parameters the HCL mixture data lies within the boundaries of its HCL components, portraying a more 'averaged' behavior. The L_F shows a decline from the *n*-octane region to the hexadecane region, which suggests a Batch Distillation or DLG mechanism. However, the \dot{m} slightly increases, likely due to the influence of dodecane, though with a different slope, indicating that the other oils were also present in the flammable gases, which in turn suggests one of the EFV mechanisms. Regardless of the burning mechanism though, the HCL mixture results show that if the individual components in a multicomponent fuel do not differ significantly, its combustion behavior is very similar to that of HCL. This implies that refined oils like diesel or gasoline could be treated as if they were HCLs for combustion purposes.

The crude oil results for the L_F and \dot{m} were in line with the T_s results, again indicating that the Batch Distillation and DLG models best describe the burning of crude oil. Both the L_F and \dot{m} quickly reach a maximum during the start of the burning and decrease steadily over time afterwards. Boilover happened for both crude oils at the end of the burning and resulted in an increase in L_F and \dot{m} (see Arai et al. (1990) and Garo et al. (1994) for more information on boilovers). As discussed in section 3.1, this data does not allow for distinguishing between the Batch Distillation and DLG model. Nevertheless, the results indicate clearly that the crude oils follow a different burning mechanism than the HCLs.

The GC spectrum of fresh REBCO and a typical REBCO residue are shown in Figure 4. Fresh REBCO consists of a considerable amount of light and medium weight hydrocarbons that were almost completely absent in the residues. Similar results were found for the GC spectra of fresh DUC and DUC residues. Overall, the crude oil residues had very different compositions from their respective fresh crudes, being depleted of the light hydrocarbon fraction and the majority of the middle hydrocarbon fraction. This trend was also found in previous studies (Buist et al., 1997; Fritt-Rasmussen et al., 2013; Garrett et al., 2000). The change in composition from fresh crude to residue indicates that the crude oils are either best described by the Imperfect EFV model or DLG model. The Batch Distillation model is less appropriate as the residue spectrum shows a gradual increase in the concentration of the heavier hydrocarbons, rather than an abrupt increase. A Batch Distillation controlled mechanism was also excluded by droplet combustion experiments with multicomponent *n*-alkane droplets, that showed the lightest component was present until the last stages of the burning (Randolph et al., 1988; Wang et al., 1984).

However, such an abrupt increase was very clear in the GC spectrum of the HCL mixture residue (Figure 5). No trace of *n*-octane was detected and only a relative concentration of 0.4% of dodecane was left in the residue, with the remaining 99.6% consisting of hexadecane. These results are very much in line with the obtained BEs of the individual species (up to 99% for *n*-octane, 98% for dodecane and 87% for hexadecane). Combined with the results from Wang et al. (1984) and Makino and Law (1988) it is therefore more likely that the residue composition is controlled by the relative BEs rather than a Batch Distillation mechanism. Similar to the crude oil data the residue composition does not match with the predictions of the EFV model and hence is best described by either the Imperfect EFV model or DLG model.

By combining the experimental results of the surface temperature, flame height, mass loss rate and residue composition (Figure 6) it becomes clear that the HCLs were best described by the EFV model, as expected. The T_s , L_F and \dot{m} remained fairly constant over time, indicating that there were no changes in gas composition and gasification rate. Deviations from this trend were most likely caused by heat losses to the water and water mass losses.

The results for the HCL mixture showed more of a mix between several models (Figure 6), which is likely caused by the close resemblance of the mixture to its individual components. The T_s increased like it did for the crude oils and suggested a DLG mechanism, which was supported by the decreasing L_F , whereas the \dot{m} showed a rather constant behavior, similar to the HCLs. The residue formation ruled out an EFV mechanism and considering the crude oil results and results from Wang et al. (1984) and Makino and Law (1988), the DLG model likely best describes the burning of mixtures with a narrow molecular weight distribution. However, an Imperfect EFV model might still predict in good approximation the burning for refined hydrocarbon mixtures like gasoline or diesel.

The crude oils, however, showed a clearly distinct burning mechanism compared to the HCLs. The increasing T_s and decreasing L_F and \dot{m} all indicated that the gasification rate changed over time as a consequence of heavier hydrocarbons contributing more to the gasification. This burning mechanism is well reflected in the REBCO residue (Figure 4), which showed a very different spectrum from the fresh crude oil. While the depletion of the lighter hydrocarbons in the residue spectrum could also indicate an Imperfect EFV mechanism, the other experimental results clearly suggested either a Batch Distillation or DLG mechanism (Figure 6). With the T_s and residue composition results being best predicted by the DLG model, the burning mechanism of crude oils is most likely dominated by diffusion-limited gasification, which indicates that

crude oils have a $Pe_m \ll 1$. This conclusion is supported by experimental work on the droplet combustion of crude oil (Ikegami et al., 2003).

From a practical point of view, a DLG mechanism means that the crude oil slick needs to continuously increase in temperature to maintain the gasification rate at the level required for self-sustainable burning. Small scale ISB experiments, compared to larger scales, might simply not be capable of reaching the temperatures required for evaporating the heaviest hydrocarbon fraction and therefore reach lower BEs, which also affects the residue composition. Without proper scaling tools, these experiments then no longer can be used to represent full scale operations, even when taking into account the regular restrictions for pool fire correlations (Babrauskas, 1983; Hottel, 1958). On the other hand, the DLG burning mechanism is rather practical for realistic ISB operations, as the large size will directly contribute to high BEs, regardless of the exact crude oil composition. Based on the maximum obtained temperature of the oil slick during the burning, combined with the hydrocarbon composition of the oil, predictions can then be made regarding the residue composition and BE. For example, the highest surface temperature recorded for the burning of REBCO was approximately 460 °C, which is close to the T_b of C_{30} . This result matched well with the composition of the residue that showed hydrocarbons up to C_{30} were reduced in concentration relative to the fresh crude oil. When the concentrations of the burned components are known, the rough BE can then be estimated.

4 Conclusions

The comparison between model predictions and experimental results for the surface temperature, flame height, mass loss rate and residue composition of HCLs and crude oils showed that multicomponent fuels burn according to a different burning mechanism than HCLs. The burning of HCLs on water showed very constant burning parameters, indicative of a constant gas composition and gasification rate, as expected of a fuel with only a single component. This type of fuel was best described by the EFV model.

The burning of the HCL mixture could be described by both the Imperfect EFV model and the DLG model. While the DLG model is likely the more accurate model, the close resemblance of the individual components allows for a reasonable approximation of the burning behavior using the Imperfect EFV model. Due to the narrow range of hydrocarbons in this mixture, it might be more representative for refined fuels, like gasoline or diesel, explaining the differences observed with the crude oils.

The changing burning parameters of the crude oils, caused by an increasing molecular weight of the evaporating hydrocarbons as the burning progresses, were best described by the Batch Distillation and DLG models. The DLG model was more accurate for the surface temperature and residue composition, indicating that crude oils burn according to a diffusion-limited gasification mechanism. This burning mechanism suggests that the residue composition, and thus the burning efficiency, is linked to the highest temperature the oil slick can acquire, which could explain the observed differences for burning efficiencies between large and small scale experiments. Based on the highest obtained surface temperature and the hydrocarbon composition of the fuel, predictions can then be made for the residue composition and burning efficiency.

5 Acknowledgements

The authors would like to thank the Danish Council for Independent research for funding the project (Grant DDF – 1335-00282). COWIfonden funded the construction of the COFA and Maersk Oil provided the crude oils that were used in this study. None of the sponsors have been involved in the results and conclusions of this paper. The authors would also like to thank Dr. Janne Fritt-Rasmussen for valuable discussions and Dr. Pierrick Mindykowski for valuable discussions and help with some of the data analysis.

6 References

- Allen, A. A. "Contained Controlled Burning of Spilled Oil During the Exxon Valdez Oil Spill", in *Proceedings of the Thirteenth Arctic and Marine Oil Spill*, Environment Canada, Ottawa, ON, 305-313, 1990.
- AMAP. "Assessment 2007: Oil and Gas Activities in the Arctic - Effects and Potential Effects", Arctic Monitoring and Assessment Programme (AMAP), Oslo, Norway, I: 423 p., 2010a.
- AMAP. "Assessment 2007: Oil and Gas Activities in the Arctic - Effects and Potential Effects", Arctic Monitoring and Assessment Programme (AMAP), Oslo, Norway, II: 277 p., 2010b.
- Arai, M., Saito, K. and Altenkirch, R. A., "A Study of Boilover in Liquid Pool Fires Supported on Water Part I: Effects of a Water Sublayer on Pool Fires", *Combustion Science and Technology*, 71(1-3): 25-40, 1990.
- Babrauskas, V., "Estimating Large Pool Fire Burning Rates", *Fire Technology*, 19(4): 251-261, 1983.
- Brandvik, P. J., Daling, P. S., Faksness, L.-G., Fritt-Rasmussen, J., Daae, R. L. and Leirvik, F. "Experimental Oil Release in Broken Ice - A Large-Scale Field Verification of Results from Laboratory Studies of Oil Weathering and Ignitability of Weathered Oil Spills.", SINTEF, Trondheim, Report no.: 26, 34 p., 2010.
- Buist, I., McCourt, J., Potter, S., Ross, S. and Trudel, K., "In Situ Burning", *Pure and Applied Chemistry*, 71(1): 43-65, 1999.
- Buist, I., Trudel, K., Morrison, J. and Aurand, D., "Laboratory Studies of the Properties of In-Situ Burn Residues", *International Oil Spill Conference Proceedings*, 1997(1): 149-156, 1997.
- Buist, I. A., Potter, S. G., Trudel, B. K., Shelnutt, S. R., Walker, A. H., Scholz, D. K., Brandvik, P. J., Fritt-Rasmussen, J., Allen, A. A. and Smith, P. "In Situ Burning in Ice-Affected Waters: State of Knowledge Report", Arctic Response Technology, Final Report 7.1.1, 293 p., 2013.
- Drysdale, D. *An Introduction to Fire Dynamics* (3rd ed.), John Wiley & Sons, Ltd., New York, 551 p., 2011.
- Farmahini Farahani, H., Shi, X., Simeoni, A. and Rangwala, A. S., "A Study on Burning of Crude Oil in Ice Cavities", *Proceedings of the Combustion Institute*, 35(3): 2699-2706, 2015.
- Fingas, M. "Introduction to Oil Chemical Analysis" in *Oil Spill Science and Technology*, M. Fingas (Ed.), Gulf Professional Publishing, Oxford, pp. 87-109, 2011a.

- Fingas, M. "Introduction to Oil Chemistry and Properties" in *Oil Spill Science and Technology*, M. Fingas (Ed.), Gulf Professional Publishing, Oxford, pp. 51-59, 2011b.
- Fingas, M. F., Li, K., Ackerman, F., Bissonnette, M. C., Lambert, P., Nelson, R., Halley, G., Campagna, P. R., Laroche, N., Jokuty, P., Turpin, R. D., Trespalacios, M. J., Belanger, J., Vanderkooy, N., Tennyson, E. J., Aurand, D. and Hiltrabrand, R. "The Newfoundland Offshore Burn Experiment - NOBE", in *In Situ Burning Oil Spill Proceedings*, National Institute of Standards and Technology and Minerals Management Service, Gaithersburg, NIST SP 857: 63-70, 1994.
- Fitzpatrick, M. "U.S. Coast Guard Arctic Pollution Response Research and Development", United States Coast Guard, Washington D.C., 3 p., 1985.
- Fritt-Rasmussen, J., Ascanius, B. E., Brandvik, P. J., Villumsen, A. and Stenby, E. H., "Composition of In Situ Burn Residue as a Function of Weathering Conditions", *Marine Pollution Bulletin*, 67(1-2): 75-81, 2013.
- Fritt-Rasmussen, J. and Brandvik, P. J., "Measuring Ignitability for In Situ Burning of Oil Spills Weathered Under Arctic Conditions: From Laboratory Studies to Large-Scale Field Experiments", *Marine Pollution Bulletin*, 62(8): 1780-1785, 2011.
- Fritt-Rasmussen, J., Brandvik, P. J., Villumsen, A. and Stenby, E. H., "Comparing Ignitability for In Situ Burning of Oil Spills for an Asphaltenic, a Waxy and a Light Crude Oil as a Function of Weathering Conditions Under Arctic Conditions", *Cold Regions Science and Technology*, 72(0): 1-6, 2012.
- Garo, J. P., Vantelon, J. P. and Fernandez-Pello, A. C., "Boilover Burning of Oil Spilled on Water", *Symposium (International) on Combustion*, 25(1): 1481-1488, 1994.
- Garrett, R. M., Guénette, C. C., Haith, C. E. and Prince, R. C., "Pyrogenic Polycyclic Aromatic Hydrocarbons in Oil Burn Residues", *Environmental Science & Technology*, 34(10): 1934-1937, 2000.
- Hottel, H. C., "Review - Certain Laws Governing Diffusive Burning of Liquids, by V. I. Blinov and G. N. Khudiakov", *Fire Research Abstracts and Reviews*, 1: 41-44, 1958.
- Ikegami, M., Xu, G., Ikeda, K., Honma, S., Nagaishi, H., Dietrich, D. L. and Takeshita, Y., "Distinctive Combustion Stages of Single Heavy Oil Droplet Under Microgravity", *Fuel*, 82(3): 293-304, 2003.
- Law, C. K., "Multicomponent Droplet Combustion With Rapid Internal Mixing", *Combustion and Flame*, 26(0): 219-233, 1976.
- Law, C. K., "Internal Boiling and Superheating in Vaporizing Multicomponent Droplets", *AIChE Journal*, 24(4): 626-632, 1978.
- Law, C. K. *Combustion Physics*, Cambridge University Press, New York, 722 p., 2006.
- Makino, A. and Law, C. K., "On the Controlling Parameter in the Gasification Behavior of Multicomponent Droplets", *Combustion and Flame*, 73(3): 331-336, 1988.

- Nordvik, A. B., "The Technology Windows-of-Opportunity for Marine Oil Spill Response as Related to Oil Weathering and Operations", *Spill Science & Technology Bulletin*, 2(1): 17-46, 1995.
- Nuka Research & Planning Group, LLC. "Oil Spill Prevention and Response in the U.S. Arctic Ocean: Unexamined Risks, Unacceptable Consequences", The PEW Environment Group, Washington, D.C., 136 p., 2010.
- Petty, S. E., "Combustion of Crude Oil on Water", *Fire Safety Journal*, 5(2): 123-134, 1983.
- Potter, S. "Test of Fire-Resistant Booms in Low Concentrations of Drift Ice - Field experiments May 2009", SINTEF, Svalbard, Report no.:27, 17 p., 2010.
- Randolph, A. L., Makino, A. and Law, C. K., "Liquid-Phase Diffusional Resistance in Multicomponent Droplet Gasification", *Symposium (International) on Combustion*, 21(1): 601-608, 1988.
- Stauffer, E., Dolan, J. A. and Newman, R. "Interpretation of Data Obtained from Neat Ignitable Liquids" in *Fire Debris Analysis*, Chap. 9, E. Stauffer, J. A. Dolan and R. Newman (Eds.), Academic Press, Burlington, pp. 295-354, 2008.
- Van Gelderen, L., Brogaard, N. L., Sørensen, M. X., Fritt-Rasmussen, J., Rangwala, A. S. and Jomaas, G., "Slick Thickness Optimization for In-Situ Burning of Crude Oil", *Fire Safety Journal*, under review, 2015.
- Wang, C. H., Liu, X. Q. and Law, C. K., "Combustion and Microexplosion of Freely Falling Multicomponent Droplets", *Combustion and Flame*, 56(2): 175-197, 1984.

Table 1. Oil characteristics

| Oil | Density at 25 °C (g/ml) ^a | Boiling point (°C) ^a | Flashpoint (°C) ^b | Viscosity at 25 °C (cP) ^a |
|------------|--------------------------------------|---------------------------------|------------------------------|--------------------------------------|
| n-Octane | 0.699 | 125-126 | 13 | 0.386 |
| Dodecane | 0.745 | 215-217 | 71 | 1.294 |
| Hexadecane | 0.770 | 287 | 135 | 3.036 |
| DUC | 0.853 | 230+ | 7 | 6.750 |
| REBCO | 0.863 | 300+ | 23 | 12.400 |

^aMeasured using an Anton Paar SVM 3000 viscometer. ^bMeasured using a Pensky-Martens Flash Point Tester: PM 4 (closed cup).

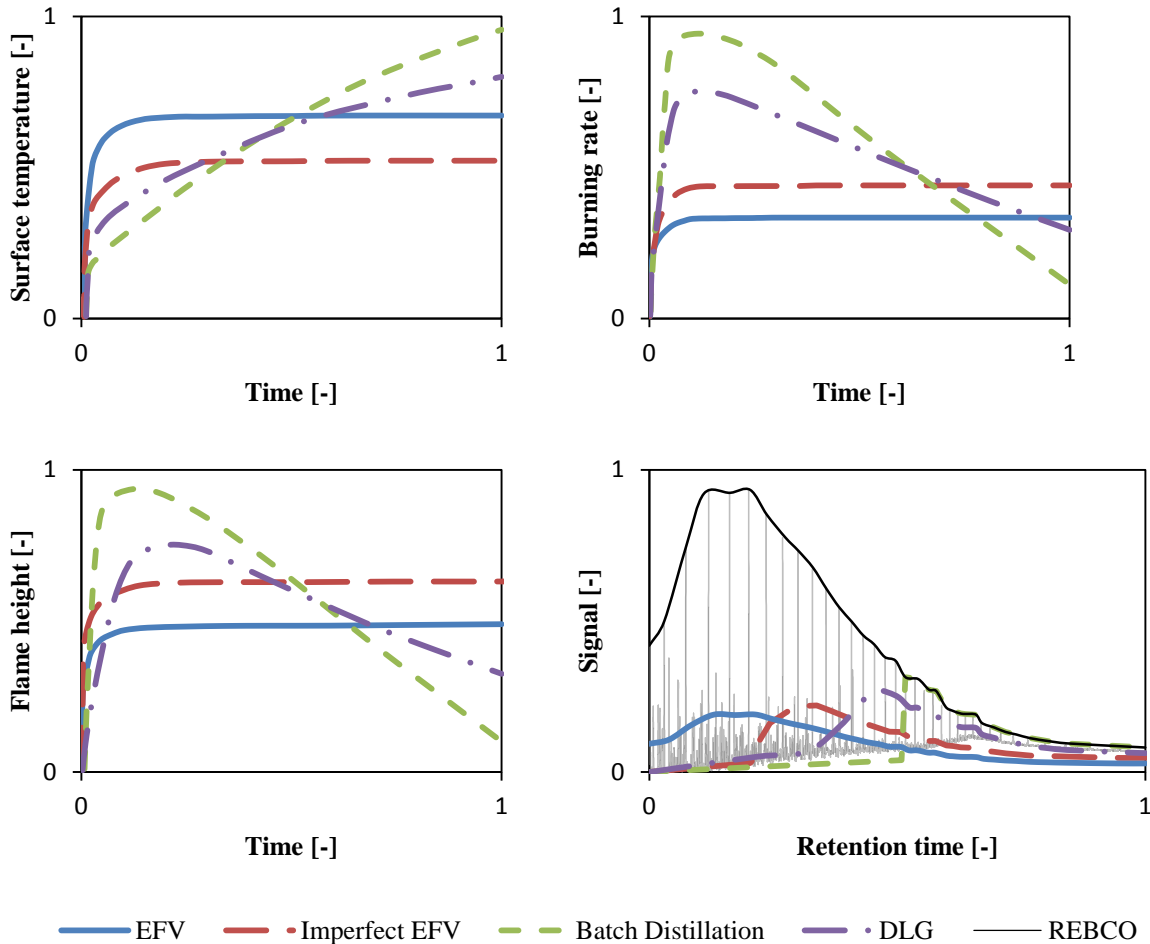


Figure 1. Crude oil combustion model predictions for the surface temperature (top left), mass loss rate (top right), flame height (bottom left) and residue composition (bottom right). The GC spectrum of REBCO was used as a reference for the model predictions.

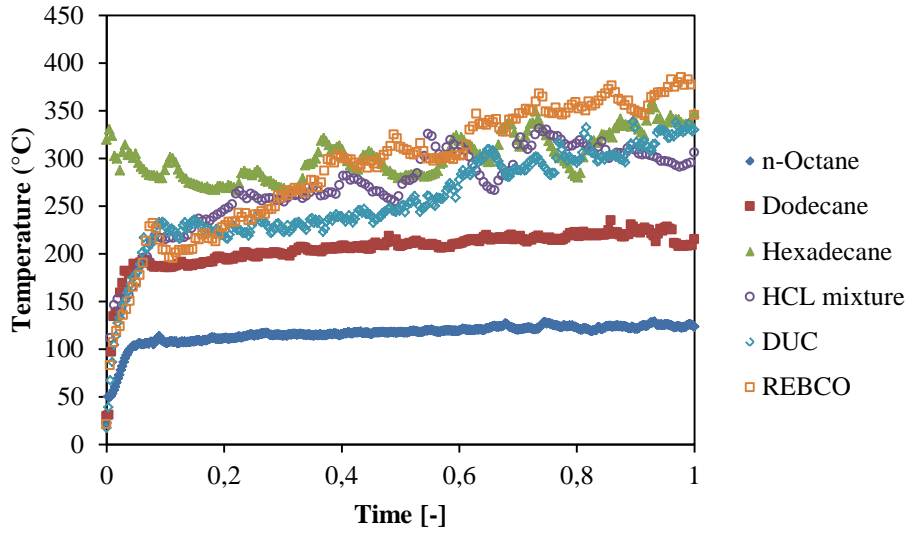


Figure 2. Surface temperatures as a function of time. Hexadecane proved difficult to ignite, hence the high temperature at ignition.

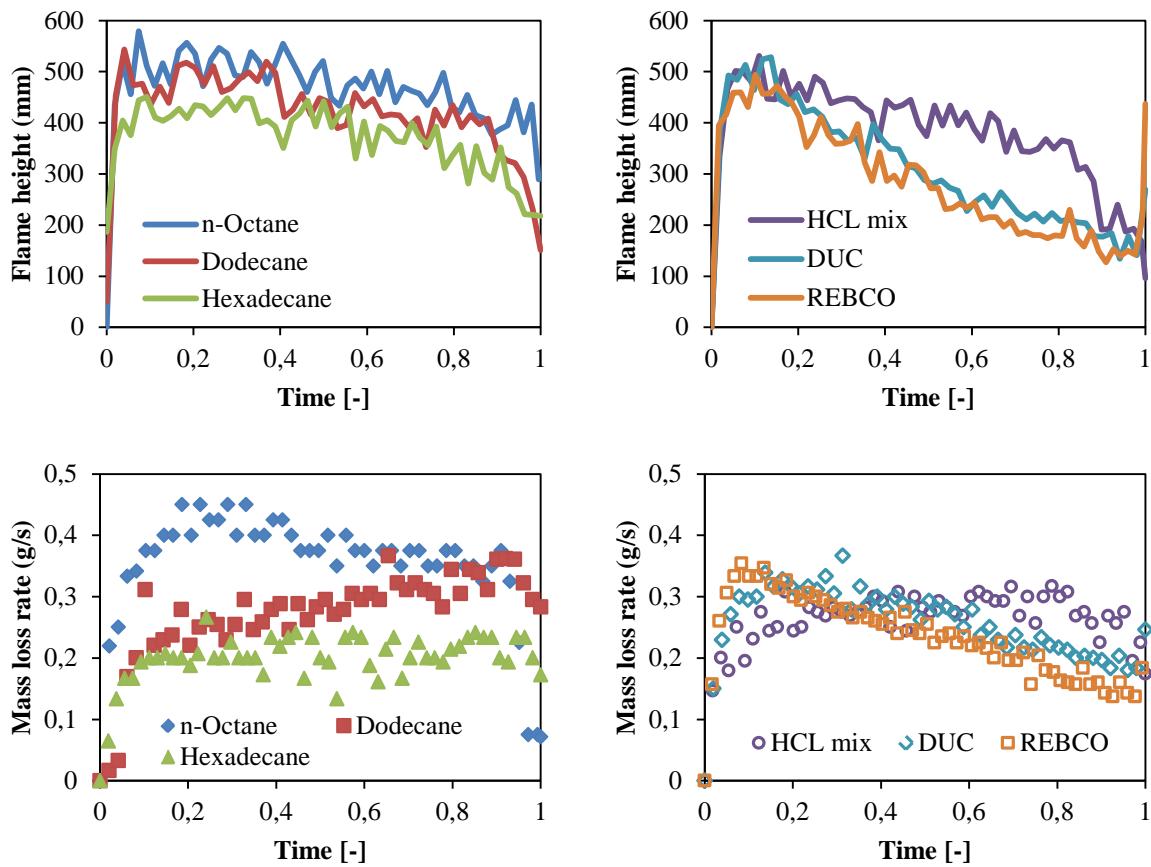


Figure 3. Flame height (top left) and mass loss rate (bottom left) as a function of time for *n*-octane, dodecane and hexadecane and flame height (top right) and mass loss rate (bottom right) for the HCL mixture, DUC and REBCO.

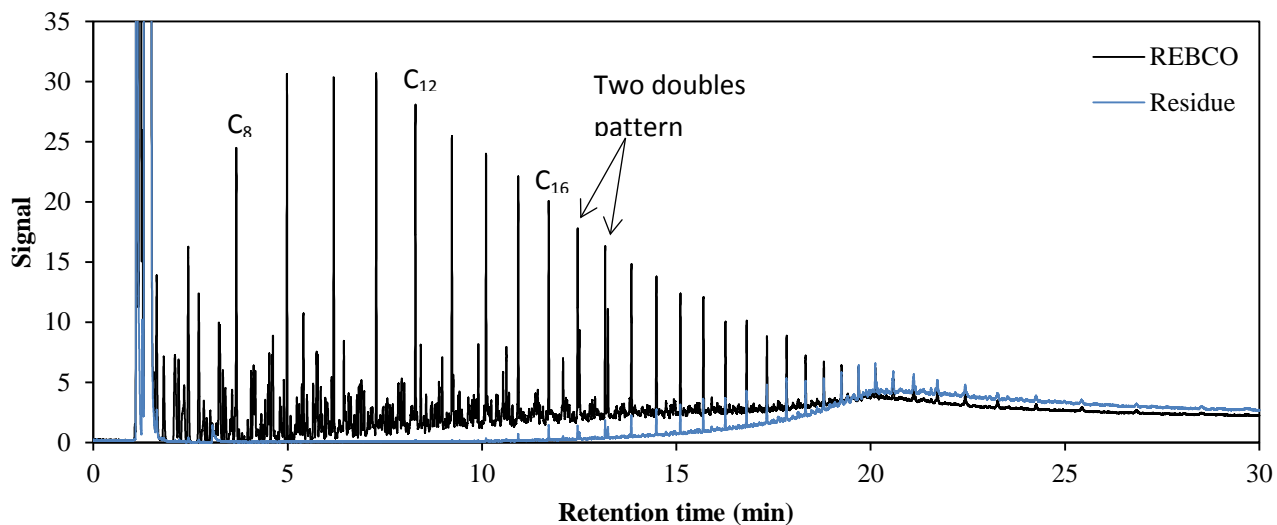


Figure 4. GC spectra of fresh REBCO and a REBCO residue. The two doubles pattern of heptadecane-pristane and octadecane-phytane as well as the peaks representing *n*-octane, dodecane and hexadecane are marked.

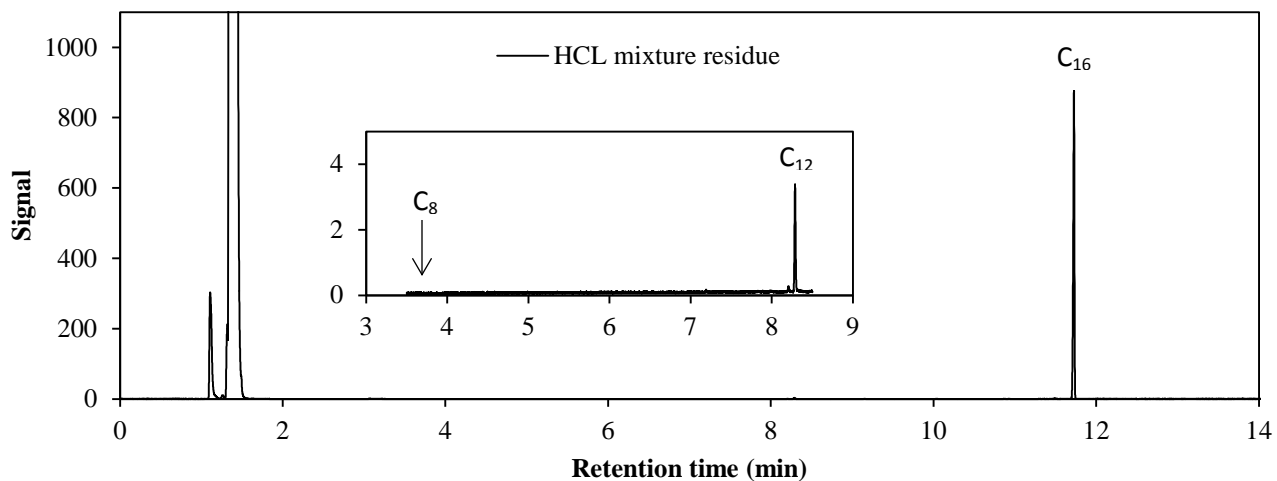


Figure 5. GC spectrum of a HCL mixture residue. The peaks representing *n*-octane, dodecane and hexadecane are marked.

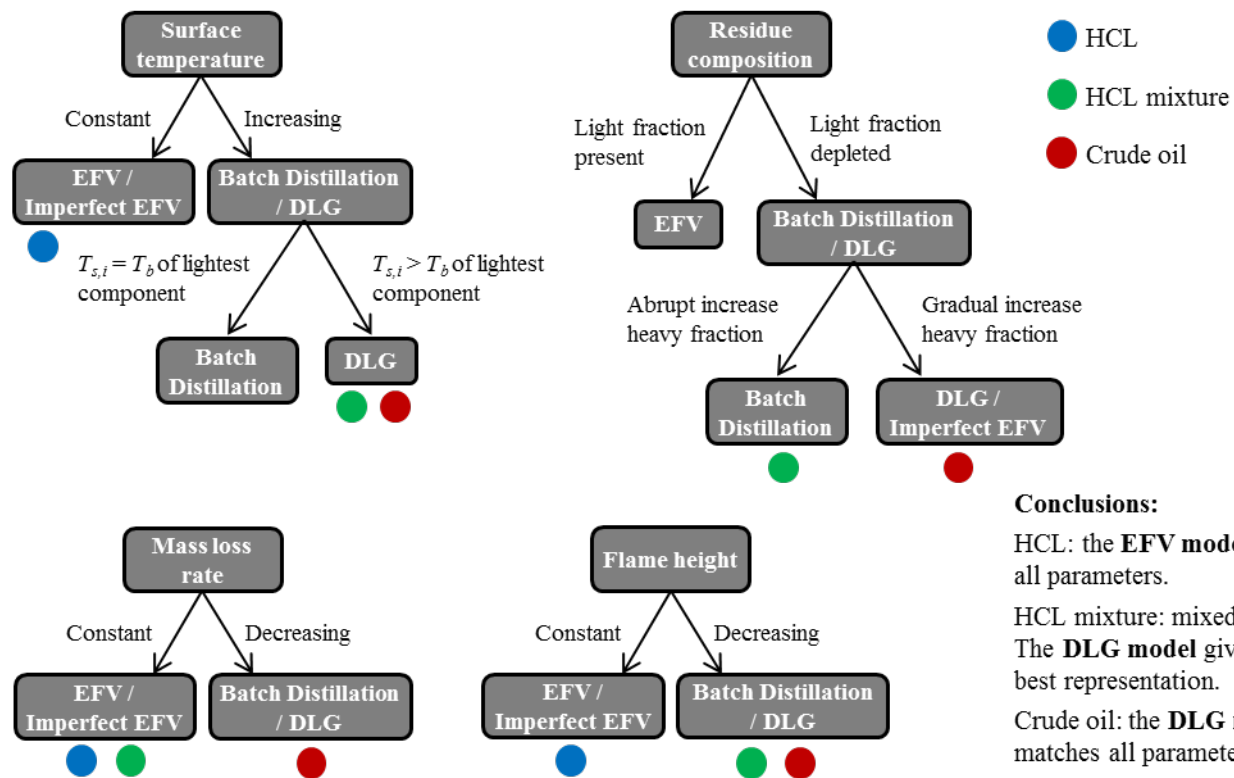


Figure 6. Model allocations for the burning mechanism of HCLs, the HCL mixture and crude oils based on four burning parameters. The colored dots represent the best model for a specific burning parameter.